

Direct Quantification of Ordering at a Solid-Liquid Interface Using Aberration Corrected Transmission Electron Microscopy

Maria Gandman,¹ Yaron Kauffmann,¹ Christoph T. Koch,² and Wayne D. Kaplan¹

¹*Department of Materials Science and Engineering, Technion-Israel Institute of Technology, Haifa 32000, Israel*

²*Institut für Experimentelle Physik, Universität Ulm, Albert-Einstein-Allee 11, 89081 Ulm, Germany*

(Received 5 August 2012; revised manuscript received 19 December 2012; published 20 February 2013)

We have used aberration corrected *in situ* transmission electron microscopy to study the interface between liquid Al and different sapphire facet planes, including quantitative analysis of the degree of residual contrast delocalization, ensuring that the experimental contrast perturbations can be associated with density perturbations in the liquid. The results confirm that the liquid is ordered at the interface, and the degree of ordering varies as a function of the sapphire facet planes, with a decreasing degree of order according to $\{0006\} > \{1\bar{2}10\} > \{10\bar{1}2\} \geq \{\bar{1}014\}$.

DOI: 10.1103/PhysRevLett.110.086106

PACS numbers: 68.08.Bc, 68.35.Rh, 68.37.Og

The investigation of ordering at solid-liquid interfaces is important for both fundamental science and many technological processes such as wetting, adhesion, solidification, crystal growth, hetero-epitaxial growth and more. Various theoretical (i.e., molecular dynamics and density functional theory simulations) [1–6], and experimental (i.e., x-ray scattering methods and transmission electron microscopy) [7–15], approaches have been used during the last half century to study ordering phenomena in liquids adjacent to crystalline surfaces. For an extensive review on this topic see Ref. [16]. While the general ordering phenomenon was predicted and experimental evidence of the phenomenon was presented, there is very little information regarding the extent of the ordering phenomenon. Moreover, the influence of specific crystalline surfaces (facets) on order in the adjacent liquid has yet to be established. We believe that establishing a correlation between the structure of the solid surface and ordering in the adjacent liquid will provide a more fundamental understanding of processes that depend on solid-liquid interfaces. As such, detailed studies of ordering in a liquid adjacent to various crystalline surface planes are required.

High resolution transmission electron microscopy (HRTEM) enables direct imaging at the atomistic level of various types of interfaces, including solid-liquid (*S-L*) interfaces. However, inherent aberrations of electromagnetic lenses (e.g., spherical aberration) in nonaberration corrected microscopes can cause significant contrast delocalization, complicating structural analysis and limiting the amount of available quantitative data. Contrast delocalization can also lead to incorrect interpretation of experimental HRTEM micrographs. Therefore, past investigations of ordering phenomena at *S-L* interfaces by HRTEM had to be combined with detailed atomistic simulations and exit wave reconstruction techniques to prove the existence of ordering [17,18]. This combined approach resulted in a successful correlation of the experimental measurements with theoretical approaches to confirm that the observed

contrast perturbations in the liquid are not an experimental artifact, and are associated with density perturbations. However, due to the complexity of this approach, ordering in liquid aluminum at Al-sapphire (α -Al₂O₃) interfaces was studied for only one facet plane (0006) of sapphire [18,19].

Contrast delocalization can be attributed to the displacement of the electron intensity $R(g)$ in the image plane. The magnitude of contrast delocalization can be described by

$$R(g) = Z\lambda g + C_s\lambda^3 g^3 + C_5\lambda^5 g^5 \quad (1)$$

where g is the spatial frequency corresponding to the periodicity of the crystal planes, Z is the defocus, λ is the electron wavelength, C_s is the third-order spherical aberration coefficient of the objective lens, and C_5 is the fifth-order spherical aberration of the objective lens. The contrast delocalization distance R can be calculated for given imaging conditions from $R = \max |R(g)|$ where $g \leq g_{\max}$, and g_{\max} is the spatial frequency corresponding to the information limit of the microscope [20,21].

The tremendous progress in the development of aberration corrected microscopes has provided a significant improvement in the spatial resolution of TEMs (i.e., sub-Angstrom resolution), and equally important has minimized contrast delocalization, and therefore provides more directly interpretable experimental data for *in situ* studies. The aberration corrector not only enables minimization of the spherical aberration of the objective system but can also be used to tune the aberrations for optimal viewing conditions using negative C_s imaging (NCSI) conditions [22]. Using the optimal defocus value for fulfilling the NCSI conditions in the C_s -corrected microscope used in the current study [23] would result in a delocalization distance of 0.25 Å, opposed to 10 Å for a typical high-voltage noncorrected microscope [24].

During *in situ* heating experiments HRTEM micrographs are not always acquired at optimal defocus due to sample drift parallel to the electron beam. Nevertheless, for cases in which the contrast delocalization distance is

smaller than the distance perpendicular to the interface of the observed contrast perturbations, direct interpretation of ordering is possible. To determine the extent of contrast delocalization, the objective lens defocus for which the micrograph was acquired must be determined. This can be accomplished using iterative methods for matching simulated micrographs of the bulk alumina with the experimental micrographs [25,26].

The goal of this study was to quantitatively study the degree of ordering at interfaces between liquid Al and sapphire, as a function of the sapphire terminating facet. We proved that aberration corrected HRTEM is an adequate tool for providing directly interpretable ordering results and used it for investigation of the general ordering phenomenon.

Since the stoichiometry of sapphire does not change in the presence of oxygen, this is a convenient material for *in situ* experiments. Moreover, at elevated temperatures and under electron beam irradiation, preferential removal of oxygen via knock-on damage results in the formation of liquid Al drops on the sapphire surface [18], providing a readily made solid-liquid interface.

TEM specimens from wafers of single crystalline α -Al₂O₃ were prepared by mechanical polishing and dimpling, followed by Ar⁺ ion milling in a Gatan precision ion polishing system. The sapphire crystals used for the specimen preparation were oriented in [10 $\bar{1}$ 0] and [1 $\bar{2}$ 10] zone axes.

The *in situ* heating experiments were conducted in a monochromated FEI Titan 80–300 S/TEM (FEI) equipped with a spherical aberration (C_s) corrector for the objective lens and operated at an accelerating voltage of 300 kV. The TEM specimens were mounted on a Gatan 652 double-tilt heating holder at 670 °C and 750 °C. For the microscope used in the current sets of experiments, the tuned C_s was checked to be stable before and after heating experiments within a maximum error of $\pm 2.5 \mu\text{m}$.

To determine the objective lens defocus for each experimental micrograph, micrographs of the sapphire (close to the interface) were compared to simulated images. The simulated images were calculated using a multislice routine, including the experimentally determined value of the microscope contrast transfer function [27]. Quantitative comparison of the simulated images and experimental micrographs was conducted using HREM-DIMA, which is a computer program based on iterative digital image matching [28]. This software combines an interactive iterative matching process via a graphical user interface and a fully quantitative comparison between experimental and simulated micrographs. The quantitative results provided the conditions (value of objective lens defocus) at which the experimental data were acquired.

Ordering in the liquid is usually described by layering and in-plane periodicity [18,19,29]. Layering is related to two-dimensional density variations in the liquid perpendicular to

the solid-liquid interface. The in-plane periodicity describes an additional degree of order within the ordered liquid layers [19]. According to previous studies, the in-plane periodicity is expected to decay faster than layering [19,29].

Assuming the intensity in the experimental micrograph is proportional to the atomic density in the sample, one can extract structural information from the contrast in the image. In the current research the layering was measured by scanning the intensity of experimental micrographs perpendicular to the solid-liquid interfaces. The in-plane periodicity was studied by constructing maps from one-dimensional Fourier transforms acquired parallel to the solid-liquid interfaces with subsequent intensity analysis of the maps [30].

The structural correlation length ξ can be used as an additional tool to quantify the amount of order at the interface [19,29]. The upper envelope of the intensity profile in the liquid can be fitted to an exponential decay

$$I(x) = a \exp\left(-\frac{x}{\xi}\right) + b \quad (2)$$

where I is the intensity profile, x is the distance from the solid, a is a normalization factor, b accounts for the background liquid density, and ξ is the correlation length at the interface. In the current study, ξ was used for quantitative comparison of ordering in liquid Al in contact with different sapphire terminating planes.

A C_s -corrected, unfiltered HRTEM micrograph of a liquid Al drop located on the (1 $\bar{2}$ 10) plane of a sapphire

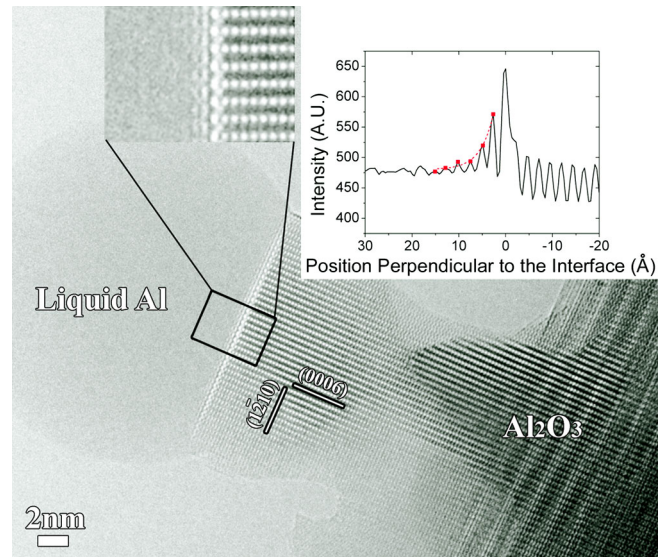


FIG. 1 (color online). C_s corrected ($C_s = -2.4 \mu\text{m}$) HRTEM micrograph of a liquid Al droplet located at the (1 $\bar{2}$ 10) surface of solid Al₂O₃. The micrograph was acquired at $T = 750 \text{ }^\circ\text{C}$. The sapphire crystal is oriented in a [10 $\bar{1}$ 0] zone axis. The inset is the intensity line scan perpendicular to the Al-Al₂O₃ interface from the region marked on the micrograph by a black rectangle. The dashed curve on the graph represents the exponential fit, from which ξ was extracted.

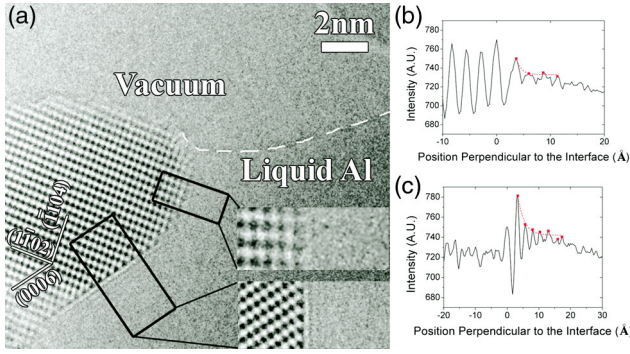


FIG. 2 (color online). (a) C_s -corrected ($C_s = -5.2 \mu\text{m}$) HRTEM micrograph of sapphire partially in contact with liquid Al. The micrograph was acquired at $T = 750^\circ\text{C}$. The sapphire is oriented in a $[1210]$ zone axis. (b) Intensity line scan perpendicular to the interface between liquid Al and the $(\bar{1}014)$ sapphire surface. (c) Intensity line scan perpendicular to the interface between liquid Al and the (0006) sapphire surface. The dashed curves on (b) and (c) represent the exponential fit, for which ξ was extracted.

whisker acquired at a nominal temperature of 750°C is presented in Fig. 1. The micrograph is from a movie that is available in the Supplemental Material [31]. The simulated image of bulk sapphire (Supplemental Material [32]) for the given acquisition conditions yielded the highest cross correlation compatibility for the objective lens defocus (Z) value of 19 nm (cross correlation of 91%). For these imaging conditions the calculated contrast delocalization distance is $5 \pm 0.4 \text{ \AA}$, and contrast perturbations beyond 5.4 \AA from the interface can be directly interpreted as density perturbations.

The ordering of liquid Al observed at the interface with sapphire is in the form of both layering and in-plane order. Six ordered layers that extend to a distance of 1.5 nm into the liquid (as measured from the sapphire edge) were detected. Partial in-plane order was found in the first four layers, extending 1 nm into the liquid [30]. $\xi = 2.76 \pm 0.47 \text{ \AA}$ ($R^2 = 0.98$, R^2 being the square of the exponential decay correlation coefficient) was determined using the exponential fit in Eq. (2).

In order to compare our results to previously published data obtained from a noncorrected microscope, ordering of liquid aluminum at the (0006) plane of sapphire was investigated. A C_s -corrected HRTEM micrograph of the interface between liquid Al and the (0006) sapphire plane acquired at 750°C is presented in Fig. 2. An additional interface between liquid Al and the $(\bar{1}014)$ sapphire plane was investigated using the same micrograph. A simulated image of the bulk sapphire resulted in the highest cross correlation for a Z value of 27 nm (cross correlation coefficient of 90%) [32].

Quantitative analysis of the ordering for liquid Al at 750°C at (0006) and $(\bar{1}014)$ sapphire planes is presented in Table I. It should be noted that no layering was found at the interface between the $(\bar{1}\bar{1}02)$ sapphire plane and vacuum [i.e., free surface of $(\bar{1}\bar{1}02)$], which thus serves as a control data set regarding the influence of residual contrast delocalization.

The results obtained for the (0006) plane at $T = 750^\circ\text{C}$ are in good agreement with the quantitative analysis presented by Kauffmann *et al.* from non- C_s -corrected HRTEM micrographs [19]. Compared to previous studies, a larger number of ordered layers was found, due to the improved resolution and detection limit of the aberration corrected TEM. The structural correlation length found in the current work is lower than the correlation length obtained in previous investigations [19]. Errors in the measurement of temperature (under the electron beam) may be responsible for the differences in ξ . In addition, the larger number of ordered layers detected in this study results in a less abrupt exponential decay, which decreases the value of the structural correlation length.

Since the use of C_s -corrected microscopy significantly simplifies the analysis of order at solid-liquid interfaces, additional experiments to probe liquid ordering as a function of temperature were conducted. An example is provided in Fig. 3, where the ordering of liquid Al at the (0006) and $(10\bar{1}2)$ planes of sapphire was investigated at 670°C . Quantitative image analysis from the bulk sapphire for the given acquisition conditions yielded a Z value of 29 nm (cross correlation of 91%).

TABLE I. Summary of the quantitative analysis of ordering of liquid Al in contact with various sapphire surfaces, as measured from the micrographs in Figs. 1–3.

Temp. ($^\circ\text{C}$)	Sapphire surface plane	Number of layers	Layering distance (\AA)	Structural correlation length ξ (\AA)	Number of layers with partial in-plane order	In-plane order distance (\AA)	Contrast delocalization distance (\AA)
750 [18,19]	(0006)	5	10	3.01 ± 0.28	3		
	(0006)	7	17	2.07 ± 0.51 ($R^2 = 0.95$)	3	8	6.1 ± 0.4
750	$(\bar{1}\bar{2}10)$	6	15	2.76 ± 0.47 ($R^2 = 0.98$)	4	10	5 ± 0.4
	$(\bar{1}014)$	4	11	0.93 ± 0.92 ($R^2 = 0.9$)	4	11	6.1 ± 0.4
670	(0006)	8	18	2.5 ± 0.32 ($R^2 = 0.98$)	3	8	6.9 ± 0.4
	$(10\bar{1}2)$	5	14	1.06 ± 0.22 ($R^2 = 0.99$)	4	11	6.9 ± 0.4

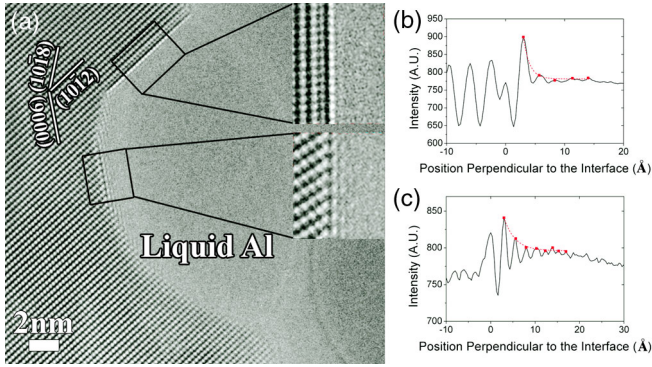


FIG. 3 (color online). (a) C_s -corrected ($C_s = -6.6 \mu\text{m}$) HRTEM micrograph of liquid Al partially confined by sapphire. The micrograph was acquired at $T = 670^\circ\text{C}$. The sapphire is oriented in a $[\bar{1}2\bar{1}0]$ zone axis. (b) Intensity line scan perpendicular to the interface of liquid Al with $\{10\bar{1}2\}$ sapphire. (c) Intensity line scan perpendicular to interface of liquid Al with $\{0006\}$ sapphire. The dashed curves in (b) and (c) represent the exponential fit, from which ξ was extracted.

The analysis of ordering of liquid Al in contact with $\{0006\}$ and $\{10\bar{1}2\}$ sapphire planes at $T = 670^\circ\text{C}$ is summarized in Table I. Interestingly, for the $\{10\bar{1}2\}$ sapphire plane the last layer of crystalline sapphire (closest to the interface) was found $2.33 \pm 0.44 \text{ \AA}$ away from the previous sapphire layer, while the interplanar spacing of this plane is 3.47 \AA . This can be attributed to relaxation at the $\{10\bar{1}2\}$ sapphire surface.

As expected, the ordering at the liquid Al- $\{0006\}$ sapphire plane at 670°C is higher than at 750°C , both in terms of the number of layers and the structural correlation length. For all the investigated solid-liquid interfaces, the ordering (both layering and in-plane order) was found to extend well beyond the maximum delocalization length. Thus for the current experimental setup the C_s -corrected *in situ* experiments can be used for direct observation of the ordering phenomenon.

The higher resolution and reduced contrast delocalization of the C_s -corrected HRTEM enabled direct investigations of the ordering phenomenon for all the investigated interfaces. This allowed for a quantitative comparison of the order in liquid Al at interfaces with different sapphire terminating facets, both in terms of the number of ordered layers and the structural correlation factor ξ . While for

most of the planes partial in-plane periodicity in the ordered Al layers was detected [30], the in-plane order values were not used for comparison of the degree of order as a function of terminating facet. The number of ordered layers in Al adjacent to the $\{0006\}$ terminating facet at 750°C is larger than the number of ordered layers adjacent to the $\{1\bar{2}10\}$ facet at the same temperature. The number of ordered layers in Al adjacent to the $\{10\bar{1}2\}$ terminating facet at 670°C is smaller than the number of ordered layers adjacent to the $\{1\bar{2}10\}$ facet at 750°C . It is logical to assume that at lower temperatures the liquid Al is more ordered (as seen for the $\{0006\}$ facet). The exact degree of order between the $\{10\bar{1}2\}$ and the $\{1\bar{1}014\}$ facets could not be determined. The structural correlation factor values support the ordered layers data (but cannot be used for more decisive conclusions due to large error values). Therefore, the decreasing degree of order as a function of sapphire terminating facet can be determined and is $\{0006\} > \{1\bar{2}10\} > \{10\bar{1}2\} \geq \{1\bar{1}014\}$. The current results regarding ordering in liquid Al at the interface with the $\{0006\}$ sapphire facet plane are in good agreement with previous studies of this system [18,19].

The comparison of ordering in liquid Al in contact with various sapphire facet planes with the periodicity of the adjacent bulk sapphire is summarized in Table II. When the d spacing of the adjacent sapphire is close to 2.87 \AA (the nearest neighbor distance in bulk liquid Al at 655°C and 750°C [33]), the distance between the ordered layers in the liquid and the in-plane periodicity mimics the periodicity of the bulk sapphire, as can be seen for planes $\{1\bar{2}10\}$ and $\{1\bar{1}014\}$. When the d spacing of the adjacent sapphire plane is less than the nearest neighbor distance in bulk liquid Al, as in the case of the $\{0006\}$ plane, the distance between ordered layers varies significantly, with values close either to the bulk sapphire d spacing or to the nearest neighbor distance in bulk liquid Al, while the in-plane periodicity still mimics the bulk sapphire. It should be noted that while the data presented in Table II for the $\{0006\}$ plane is at 750°C , the distance between ordered layers in liquid adjacent to the $\{0006\}$ plane is similar for both 750°C and 670°C . For the case of the $\{10\bar{1}2\}$ terminating plane, the sapphire d spacing is significantly larger than the nearest neighbor distance in bulk liquid Al, and the distance between the ordered layers in the liquid was measured to be identical (within the measurement error)

TABLE II. Ordering in liquid Al adjacent to sapphire terminating planes, compared to the sapphire interplanar distance.

Temperature ($^\circ\text{C}$)	Plane	d spacing of bulk sapphire (\AA)	Distance between ordered layers in liquid (\AA)	In-plane periodicity in bulk sapphire (\AA)	In-plane periodicity in liquid adjacent to the sapphire plane (\AA)
750	$\{0006\}$	2.165	$2 - 3(\pm 0.44)$	4.2	4.2
	$\{1\bar{2}10\}$	2.37	$2.22 - 2.66(\pm 0.44)$	2.27	2.27
	$\{1\bar{1}014\}$	2.55	$2.3 - 2.7(\pm 0.44)$	3.6	3.6
670	$\{10\bar{1}2\}$	3.48	$2.7 - 3(\pm 0.44)$	2.6	~ 4

to the nearest neighbor distance in the bulk liquid. The in-plane periodicity differed both from the bulk sapphire and from bulk liquid Al. It is important to note that the last (closest to the solid-liquid interface) layer of the (10 $\bar{1}$ 2) sapphire plane was found to be relaxed in comparison to bulk sapphire.

The nearest neighbor distance in liquids is the mean distance between nearest atoms of bulk liquid (in three dimensions). By constraining the atoms into two-dimensional layers, the layering phenomenon creates an additional degree of order. From the analysis presented above, for the current system it can be concluded that when the bulk periodicity of the crystalline phase is close to the nearest neighbor distance of the bulk liquid, the periodicity of the ordered liquid layers mimics the periodicity of the bulk crystal. However, when the crystalline periodicity is significantly larger than the nearest neighbor distance in the bulk liquid, the distance between liquid layers reduces to the nearest neighbor distance of the bulk liquid.

It should be noted that in the current study the ordering phenomenon was measured in terms of overall contrast perturbations at the solid-liquid interface. Opposed to a previous study [34], we believe that no conclusions regarding the composition at the interface can be drawn from *in situ* HRTEM micrographs without experimental corroboration from additional techniques.

In conclusion, we have shown that *in situ* C_s -corrected HRTEM provides a powerful tool for direct analysis of the ordering phenomenon at solid-liquid interfaces. Implementation of the current experimental setup enabled us to detect order on every examined solid-liquid interface, showing that for the sapphire-Al solid-liquid system, the ordering phenomenon is general, while the degree of order is influenced by the nature of the sapphire terminating plane.

-
- [1] F. Spaepen, *Acta Metall.* **23**, 6 (1975).
 [2] F.F. Abraham and Y. Singh, *J. Chem. Phys.* **67**, 5 (1977).
 [3] A. Hashibon, J. Adler, M. W. Finnis, and W.D. Kaplan, *Comput. Mater. Sci.* **24**, 4 (2002).
 [4] D. Buta, M. Asta, and J. J. Hoyt, *Phys. Rev. E* **78**, 3 (2008).
 [5] A. Kyrilidis and R. A. Brown, *Phys. Rev. E* **51**, 6 (1995).
 [6] K. Joongoo, Z. Junyi, C. Curtis, D. Blake, G. Glatzmaier, K. Yong-Hyun, and W. Su-Huai, *Phys. Rev. Lett.* **108**, 22 (2012).
 [7] S. H. Oh, M. F. Chisholm, Y. Kauffmann, W. D. Kaplan, W. Luo, M. Rühle, and C. Scheu, *Science* **330**, 489 (2010).
 [8] M. Baram, Stephen H. Garofalini, and W. D. Kaplan, *Acta Mater.* **59**, 14 (2011).
 [9] R. G. Horn and J. N. Israelachvili, *J. Chem. Phys.* **75**, 3 (1981).
 [10] C. J. Yu, A. G. Richter, A. Datta *et al.*, *Phys. Rev. Lett.* **82**, 11 (1999).
 [11] C.-J. Yu, A. G. Richter, J. Kmetko *et al.*, *Phys. Rev. E* **63**, 2 (2001).
 [12] M. F. Reedyk, J. Arsic, F. K. de Theije, M. T. McBride, K. F. Peters, and E. Vlieg, *Phys. Rev. B* **64**, 3 (2001).
 [13] M. F. Reedyk, J. Arsic, F. F. A. Hollander, S. A. de Vries, and E. Vlieg, *Phys. Rev. Lett.* **90**, 6 (2003).
 [14] F. Grey, R. Feidenhans'l, J. Skov Pedersen, M. Nielsen, and R. L. Johnson, *Phys. Rev. B*: **41**, 13 (1990).
 [15] W. J. Huisman, J. F. Peters, M. J. Zwanenburg, S. A. de Vries, T. E. Derry, D. Abernathy, and J. F. van der Veen, *Nature (London)* **390**, 6658 (1997).
 [16] W. D. Kaplan and Y. Kauffmann, *Annu. Rev. Mater. Res.* **36**, 1 (2006).
 [17] S. E. Donnelly, R. C. Birtcher, C. W. Allen, I. Morrison, K. Furuya, M. Song, K. Mitsuishi, and U. Dahmen, *Science* **296**, 507 (2002).
 [18] S. H. Oh, Y. Kauffmann, C. Scheu, W. D. Kaplan, and M. Rühle, *Science* **310**, 5748 (2005).
 [19] Y. Kauffmann, S. H. Oh, C. T. Koch, A. Hashibon, C. Scheu, M. Rühle, and W. D. Kaplan, *Acta Mater.* **59**, 11 (2011).
 [20] H. Lichte, *Ultramicroscopy* **38**, 1 (1991).
 [21] M. Lentzen, *Microsc. Microanal.* **14**, 16 (2008).
 [22] C. L. Jia, M. Lentzen, and K. Urban, *Microsc. Microanal.* **10**, 2 (2004).
 [23] See Supplemental Material at <http://link.aps.org/supplemental/10.1103/PhysRevLett.110.086106> for information on the details of our NCSI conditions.
 [24] See Supplemental Material at <http://link.aps.org/supplemental/10.1103/PhysRevLett.110.086106> for information on the delocalization distance for a high-voltage noncorrected TEM.
 [25] G. Mobus and M. Rühle, *Ultramicroscopy* **56**, 1 (1994).
 [26] G. Mobus, A. Levay, B. J. Inkson, M. J. Hytch, A. Trampert, and T. Wagner, *Z. Metallk. D.* **94**, 4 (2003).
 [27] P. A. Stadelmann, *Ultramicroscopy* **21**, 2 (1987).
 [28] Y. Kauffmann, <http://tx.technion.ac.il/~mtyaron/HREM-DIMA.html>.
 [29] A. Hashibon, J. Adler, M. W. Finnis, and W. D. Kaplan, *Interface Sci.* **9**, 3 (2001).
 [30] See Supplemental Material at <http://link.aps.org/supplemental/10.1103/PhysRevLett.110.086106> for investigation of layering and in-plane periodicity.
 [31] See Supplemental Material at <http://link.aps.org/supplemental/10.1103/PhysRevLett.110.086106> for a movie of the moving droplet.
 [32] See Supplemental Material at <http://link.aps.org/supplemental/10.1103/PhysRevLett.000.000000> for simulated images of bulk sapphire in Figs. 1–3.
 [33] R. R. Fessler, R. Kaplow, and B. L. Averbach, *Phys. Rev.* **1**, 1 (1966).
 [34] S. B. Lee and Y. M. Kim, *Acta Mater.* **59**, 1383 (2011).